

The Sensitivity of Mountain Snowpack Accumulation to Climate Warming

JUSTIN R. MINDER

Department of Atmospheric Sciences, University of Washington, Seattle, Washington

(Manuscript received 28 May 2009, in final form 17 December 2009)

ABSTRACT

Controls on the sensitivity of mountain snowpack accumulation to climate warming (λ_S) are investigated. This is accomplished using two idealized, physically based models of mountain snowfall to simulate snowpack accumulation for the Cascade Mountains under current and warmed climates. Both models are forced from sounding observations. The first model uses the linear theory (LT) model of orographic precipitation to predict precipitation as a function of the incoming flow characteristics and uses the sounding temperatures to estimate the elevation of the rain–snow boundary, called the melting level (ML). The second “ML model” uses only the ML from the sounding and assumptions of uniform and constant precipitation. Both models simulate increases in precipitation intensity and elevated storm MLs under climate warming. The LT model predicts a 14.8%–18.1% loss of Cascade snowfall per degree of warming, depending on the vertical structure of the warming. The loss of snowfall is significantly greater, 19.4%–22.6%, if precipitation increases are neglected. Comparing the two models shows that the predominant control on λ_S is the relationship between the distribution of storm MLs and the distribution of topographic area with elevation. Although increases in precipitation due to warming may act to moderate λ_S , the loss of snow accumulation area profoundly limits the ability of precipitation increases to maintain the snowpack under substantial climate warming (beyond 1°–2°C). Circulation changes may act to moderate or exacerbate the loss of mountain snowpack under climate change via impacts on orographic precipitation enhancement.

1. Introduction

Mountain snow maintains glaciers, sets the extent of ecosystems, provides for recreation, and produces major hazards in the form of avalanches. Mountain snowpack is crucial for many communities because it preserves the precipitation that falls during wintertime storms and releases it as runoff, which provides water resources during dry summer months. Globally about one-sixth of the world’s population relies on glaciers and seasonal snow and ice for water resources, much of which resides in mountainous terrain (Barnett et al. 2005).

The importance of mountain snow and its intimate connections to climate have spurred recent research into how it is affected by climate change and variability. A focal point for these studies has been the mountains of the western United States, where snowpack makes a large contribution to regional hydrology and is heavily relied upon for water resources (e.g., Serreze et al. 1999;

Barnett et al. 2005). Observations show a regionwide decline in spring snowpack since the mid-1900s, dominated by loss at low elevations where wintertime temperatures are near freezing (Mote et al. 2005). These losses have been attributed to increased temperatures (Mote et al. 2005; Hamlet et al. 2005; Mote 2006; Mote et al. 2008), which lead to snow loss via some combination of increased frequency of rain versus snow (Knowles et al. 2006) and increased wintertime melting (Mote et al. 2005). Complicating the picture is large year-to-year variability. Interannual variability of springtime snowpack comes largely from variability of wintertime precipitation (Cayan 1996; Hamlet et al. 2005; Mote et al. 2008), which is in turn related to the variability of key patterns of atmospheric circulation (Cayan 1996; Mote et al. 2008; Stoelinga et al. 2010). These natural fluctuations make it challenging to quantify trends with confidence, to extrapolate observed changes to project future climate, or to clearly discern changes in snowpack due to anthropogenic warming trends (e.g., Mote et al. 2008; Casola et al. 2009; Stoelinga et al. 2010). For instance, it is only recently that changes in the western United States snowpack have been formally detected and attributed to anthropogenic climate change, in an effort that required

Corresponding author address: Justin Minder, Dept. of Atmospheric Sciences, Box 351640, University of Washington, Seattle, WA 98105.

E-mail: juminder@atmos.washington.edu

synthesis of extensive station observations with hundreds of years of model integrations (Pierce et al. 2008).

Other research in the western United States has focused on making projections of snowpack for the coming century by using global climate models (GCMs) to force comprehensive regional models of mountain climate and hydrology (e.g., Hamlet and Lettenmaier 1999; Leung and Qian 2003; Vicuna et al. 2007; Salathé et al. 2008; Climate Impacts Group 2009). However, despite the advanced techniques used, projections of future snowpack from these models are still fraught with uncertainty. Much of the uncertainty is inherited from the climate projections of the parent GCMs used to force them, while further uncertainties stem from the sensitivity of regional models to how key physical processes are parameterized.

To minimize the previously mentioned challenges presented by natural variability and modeling uncertainties, this paper takes a different approach to understanding how climate change affects mountain snowpack. In particular, a pair of idealized, physically based models is used to simulate snowfall for the Cascade Mountains. Experiments with these models are then used to study the changes in climatological snow accumulation occurring because of local changes in temperature alone.

2. Focus and strategy

This paper examines the physical controls on the sensitivity of mountain snowpack to local temperature changes (e.g., Casola et al. 2009). Here, Σ_t is defined as a measure of the total snow liquid water equivalent (SWE) integrated over some region (e.g., the annual accumulated SWE integrated over a catchment, measured in units of volume), and T is a representative surface temperature (e.g., the mean surface temperature at sea level). The temperature sensitivity of the snowpack is then defined as

$$\lambda \equiv \frac{1}{\Sigma_t} \frac{d\Sigma_t}{dT}. \quad (1)$$

Unless otherwise noted, values of λ quoted are normalized by the Σ_t associated with the control climate such that they represent percentage changes in the snowpack per degree of warming. Here, λ can be expanded into the direct and indirect effects of warming:

$$\lambda \approx \frac{1}{\Sigma_t} \left(\frac{\partial \Sigma_t}{\partial T} + \sum_i \frac{\partial \Sigma_t}{\partial y_i} \frac{\partial y_i}{\partial T} \right). \quad (2)$$

The direct sensitivity $\partial \Sigma_t / \partial T$ is due to changes in precipitation phase and melting directly attributable to warming. Indirect sensitivities $(\partial \Sigma_t / \partial y_i)(\partial y_i / \partial T)$ include changes in a related variable y_i that in turn affect snow accumulation (e.g., changes in precipitation intensity due to warming

that in turn affect snowfall). This paper only considers indirect sensitivities that are closely tied to local changes in temperature. For instance, changes in snowpack due to possible global warming induced changes in midlatitude storm tracks are neglected.

Casola et al. (2009) used three methods to determine λ for the portion of the Cascade Mountains draining into Puget Sound (Fig. 1): a simple geometrical model daily station observations of precipitation and temperature, and a sophisticated hydrological model. In estimating the direct sensitivity ($\partial \Sigma_t / \partial T$, neglecting precipitation changes) all three methods yielded remarkably similar values of between 22% and 24% loss of 1 April SWE per degree of warming. The agreement between methods suggests that λ is a robust measure that is determined largely by relatively simple controls. An alternative, observationally based estimate of the direct sensitivity of Cascade snowpack gives a lower value of 15% °C⁻¹ (Stoelinga et al. 2010). Other studies have estimated λ values between -6% and -10% °C⁻¹ for the California Sierra Nevada (Howat and Tulaczyk 2005) and equal to approximately -15% °C⁻¹ for the Swiss Alps (Beniston et al. 2003, reported as -30% for 2°C of warming).

In examining λ , this study considers the sensitivity of mountain precipitation intensity to warming. This indirect sensitivity has not been addressed in detail in other studies of λ (e.g., Howat and Tulaczyk 2005; Casola et al. 2009). However, significant precipitation increases may occur over many mid- and high-latitude mountains under climate warming. GCMs suggest that global-mean precipitation will increase by 2%–3% per degree of warming (e.g., Held and Soden 2006) and that precipitation intensity will increase throughout most of the mid- and high latitudes (e.g., Tebaldi et al. 2006). Although GCMs cannot adequately resolve the dominant scales of mountain precipitation, simple theories (e.g., Sawyer 1956; Smith 1979; Smith and Barstad 2004) predict that, under neutral stratification, orographic precipitation intensity is proportional to the low-level moisture flux impinging on a mountain. This suggests that if the relative humidity (RH) and winds do not change with warming, then low-level moisture fluxes, and hence orographic precipitation, might scale according to the Clausius–Clapeyron (CC) relationship at ~6%–7% °C⁻¹ of warming. Using high-resolution numerical simulations, Kirshbaum and Smith (2008) showed that increased temperature and moisture flux do indeed lead to robust increases in orographic precipitation. However, they also showed that precipitation does not increase with temperature as fast as the moisture flux, due to both thermodynamic and microphysical effects.

In this study, a pair of idealized, physically based models of the climatology of snowpack accumulation is

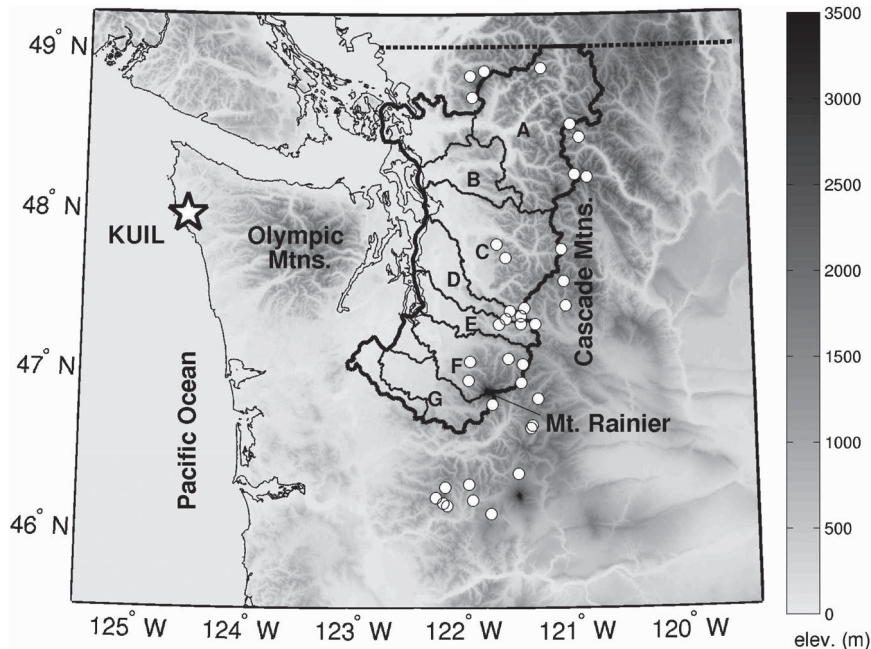


FIG. 1. Map of study region. Topography of the Cascades and Olympic Mountains is shown in grayscale (maximum elevation is 4392 m at Mount Rainier). The boundary of the catchment that drains the Cascades into the Puget Sound (with the exception of a small section in Canada, United States–Canadian border is dashed) is shown with a thick line. Major catchments within that basin are delineated with narrow lines (those used for Fig. 9 are labeled A–G). The location of KUIL is shown with a star, and the locations of SNOTEL stations used in Fig. 9 are shown with white circles.

used to determine the controls on λ . These models are favored for their efficiency (which allows for a large number of experiments), their adaptability (which allows for substantial changes in model physics and forcing data), and their simplicity (which allows fundamental processes to be clearly diagnosed). For precisely determining the value of λ these models may not be superior to observational techniques and complex models. However, the use of simple models allows for the formulation of controlled experiments and analyses to isolate controls on λ , which would not be possible with other methods. This study only considers snowpack changes associated with changes in snow accumulation. This is referred to as the temperature sensitivity of the snowfall λ_S . This differs from the full sensitivity of the snowpack λ because it neglects the effects of increases in temperature on snow ablation. The present study focuses on Washington State's Cascade Mountains but will also arrive at some general lessons about midlatitude mountain snowpack and climate.

The outline of the paper is as follows: First, an intermediate complexity model of mountain snowfall is described and used to estimate λ_S for the Cascades as well as the relative importance of precipitation and melting level (ML) changes. Then a simpler model is developed to reveal the fundamental controls on λ_S . Next

a series of experiments is presented to quantify the topographic and climatic controls on changes in mountain snowfall. Last, the main conclusions are summarized.

3. Linear theory orographic snowfall model

A model that accounts for many of the fundamental physical processes that shape the distribution of orographic snowfall serves as the starting point for this investigation. The model predicts snowfall on a storm-by-storm basis as a function of the characteristics of the incoming flow and includes the following: 1) spatial variability in precipitation; 2) storm-to-storm variability in precipitation intensity; 3) the dependence of the surface rain–snow transition on the upstream MLs; and 4) the temperature dependence of both orographic precipitation intensity and storm ML. Although it includes all of these aspects, the model is also simple enough that the controls on λ_S can be clearly discerned.

a. Methods

The model for orographic snowfall presented in this section has its foundation in the linear theory (LT) model of orographic precipitation (Smith and Barstad

2004). The LT model solves for the steady-state condensation, advection, fallout, and evaporation of water occurring in vertically integrated atmospheric columns for given uniform (horizontally and vertically) and constant impinging flow. The model assumes stable stratification and saturated conditions. It solves linearized equations of motion for flow over topography to represent the pattern of ascent responsible for the generation of orographic clouds. It also accounts for the finite time that is required for cloud water to convert into precipitation and the time it takes for precipitation to fall to the ground, allowing for the downwind drift of cloud and precipitation. Additionally, it contains a representation of lee-side evaporation that suppresses precipitation downwind of terrain.

The LT model is run by prescribing characteristic wind speed and direction, stratification (moist stability N_m), and low-level temperatures (which determine the specific humidity), as well as two microphysical time-delay constants, τ_c and τ_f , representing time scales for the conversion of cloud to precipitation and fallout, respectively, and a background precipitation rate P_{bg} , representative of precipitation generated directly by synoptic storms. The model has a simple formulation in Fourier space, allowing for rapid computation of solutions at high spatial resolution. The LT model, when properly calibrated, has proven remarkably skillful, particularly for climatological applications (e.g., Smith et al. 2003; Barstad and Smith 2005; Anders et al. 2007; Crochet et al. 2007). For instance, over the Olympic Mountains, just west of the Cascades (Fig. 1), the LT model has been shown to produce realistic precipitation patterns when compared with a dense network of gauges and a high-resolution atmospheric model (Anders et al. 2007).

For this study the LT model is first used to simulate the climatology of total precipitation over the Cascades. The model is run at approximately 1-km horizontal resolution, with the bottom boundary condition provided by the National Elevation Dataset 1-arc-s Digital Elevation Model (available online at <http://ned.usgs.gov/>) coarsened to 30-arc-s resolution. The LT model is forced using rawinsonde measurements taken twice daily (0000 and 1200 UTC) at Quillayute (KUIL), Washington, between 1980 and 2007 (location shown in Fig. 1). Conditions likely to correspond to mountain precipitation events are isolated by picking out “storm” soundings, defined as soundings where the 1–2-km layer has average wind direction between 160° and 330° and average RH greater than 85%. Temperature forcing comes from the lowest level in the sounding, and wind forcing is the vector-averaged winds from the 1–2-km layer. The moist stability forcing N_m is also calculated from the 1–2-km layer by first calculating the profile of N_m^2 [using Eq. (36) from

Durran and Klemp (1982)], averaging it over the layer, and then taking the square root. The microphysical time delays τ_c and τ_f are set equal to each other (τ) following Smith and Barstad (2004). Both τ and P_{bg} , which are not directly observable, are reserved as tunable parameters.

When the flow is unstably stratified ($N_m^2 < 0$), the LT model cannot solve for the airflow dynamics. Observations (not shown) from a network of gauges in the Olympic Mountains near the KUIL sounding (described by Anders et al. 2007 and Minder et al. 2008) show that approximately 25% of precipitation falls when the upstream sounding indicates unstable conditions ($N_m^2 < 0$ for the 1–2-km layer). This is taken as an indication that unstable events cannot be neglected in the climatology. Accordingly, these events are included, albeit rather crudely, by simply setting N_m equal to zero for moderately unstable soundings.

After using the LT model to predict the pattern of precipitation, the temperature structure from the KUIL sounding is used to predict the pattern of precipitation phase (rain versus snow) on a storm-by-storm basis. For each event the sounding is used to determine the ML upwind of the mountain as the lowest elevation where the sounding temperature crosses a 1°C threshold. This threshold roughly corresponds to the temperature where 50% of the time precipitation falls as snow, according to results of U.S. Army Corps of Engineers (1956) and Dai (2008) for a site in the California Sierra Nevada and for a global dataset of land observations, respectively. As mentioned earlier, the LT model assumes a saturated sounding with uniform moist stability. For consistency with these assumptions the ML is calculated from an idealized version of the sounding, constructed with the observed 1.5-km temperature and the N_m used to force the model.

It is common for the 0°C isotherm, radar bright band, and ML to dip to lower elevations on the mountainside (sometimes exceeding 500 m displacement) than in the free air upstream of the mountains (Marwitz 1987; Medina et al. 2005; Lundquist et al. 2008). The LT snowfall model accounts for this effect by introducing a constant orographic ML depression ΔML , the value of which is used as a tunable parameter.

To warm the LT snowfall model for climate change experiments, a new idealized sounding is constructed with the 1.5-km temperature warmed by 1°C and the same uniform N_m as used in the control simulation. This results in warming that is a function of elevation, with less warming at 0 km (on average 0.83°C instead of 1°C). This methodology is motivated by the expectation of a roughly constant midlatitude moist stability under climate change (Frierson 2006). The surface temperature

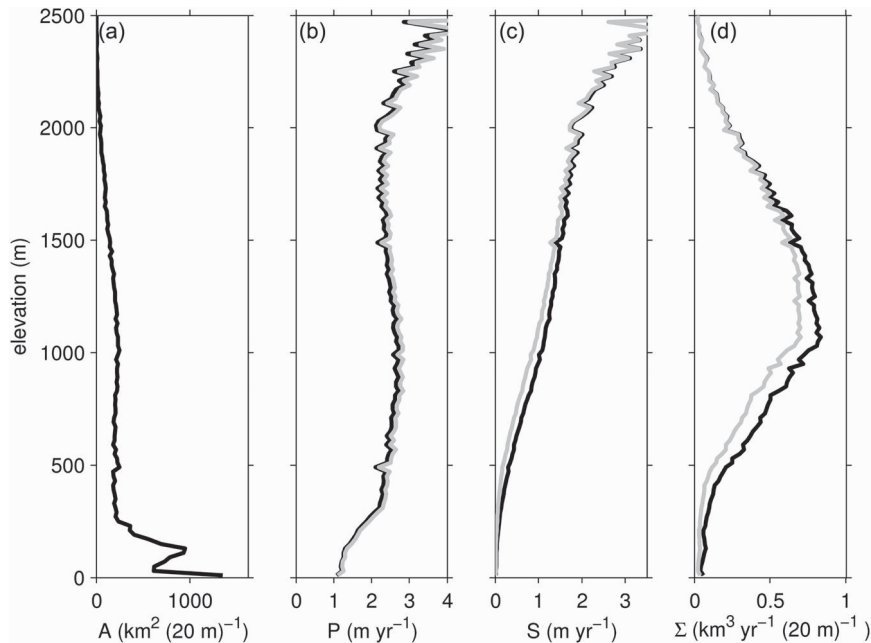


FIG. 2. Profiles of LT snowfall model variables for the Puget Sound catchment (Fig. 1) from the *climo_control* run: (a) topographic area $A(z)$, (b) average accumulated precipitation $P(z)$, (c) average snow water accumulation $S(z)$, and (d) integrated snow water accumulation $\Sigma(z)$. Control simulation is shown in black, and gray lines are for simulation with 1.5-km level warmed by 1°C (surface warming of 0.83°C).

and MLs used for the warmed simulations are attained from the new sounding.

b. Results

A description of the calibration and evaluation of the LT snowfall model is given in appendices A and B. The LT model is first used to simulate snowpack accumulation over the Cascades under current and warmed climate conditions for the 28-yr period 1980–2007. Here, λ_S is calculated by dividing the modeled fractional Σ_T changes by the average surface warming (0.83°C).

Results are plotted as profiles in Fig. 2, including the distribution with elevation of the following: topographic area (the derivative of the hypsometric curve) $A(z)$; average annual precipitation $P(z)$; water equivalent snowfall $S(z)$; and annual-mean total volume of accumulated snow water $\Sigma(z) = A(z) \times S(z)$. Note that the largest volume of snow Σ accumulates at midelevations (Fig. 2d), where snowfall is frequent and large amounts of topographic area reside.

In the warmed simulation, precipitation increases at all elevations (Fig. 2b) but not enough to offset the reduced frequency of snowfall due to shifts in the ML (Fig. 2c). Maps of the change in precipitation and snowfall are plotted in Fig. 3. The precipitation increases uniformly by approximately $5\% \text{ }^{\circ}\text{C}^{-1}$. The change in snowfall is variable

in space and is negative everywhere except the highest volcanic peaks.

Integrating the $\Sigma(z)$ curves for the control and warmed climates and taking a fractional difference yields a λ_S of $-18.1\% \text{ }^{\circ}\text{C}^{-1}$ (Table 1, *climo_control*). Isolating the effects of ML changes, by holding modeled precipitation constant, gives a sensitivity of $-22.6\% \text{ }^{\circ}\text{C}^{-1}$, which will be referred to as λ_{ML} ; thus, precipitation changes reduce the magnitude of the sensitivity of snow accumulation by $4.5\% \text{ }^{\circ}\text{C}^{-1}$. Changes in precipitation alone give a sensitivity of $5.49\% \text{ }^{\circ}\text{C}^{-1}$ ($\sim 1\% \text{ }^{\circ}\text{C}^{-1}$ less than the CC scaling), which will be referred to as λ_P .

Interestingly, the full sensitivity is not equal to the sum of the partial sensitivities to ML and precipitation changes ($\lambda_S \neq \lambda_{\text{ML}} + \lambda_P$)—only 82% of the increased precipitation is realized as an increase in snowfall. The explanation for this is purely geometrical. Although precipitation intensity for each storm is increased by several percent across the basin, some of the increase occurs in regions that receive snow in the control climate but rain in the warmed climate, meaning it is lost as runoff.

The λ_{ML} value of $-22.6\% \text{ }^{\circ}\text{C}^{-1}$ from the LT snowfall model is within the range of the λ values attained by Casola et al. (2009) when they neglected precipitation changes (from -22% to $-24\% \text{ }^{\circ}\text{C}^{-1}$). However, comparison of these estimates is not entirely straightforward

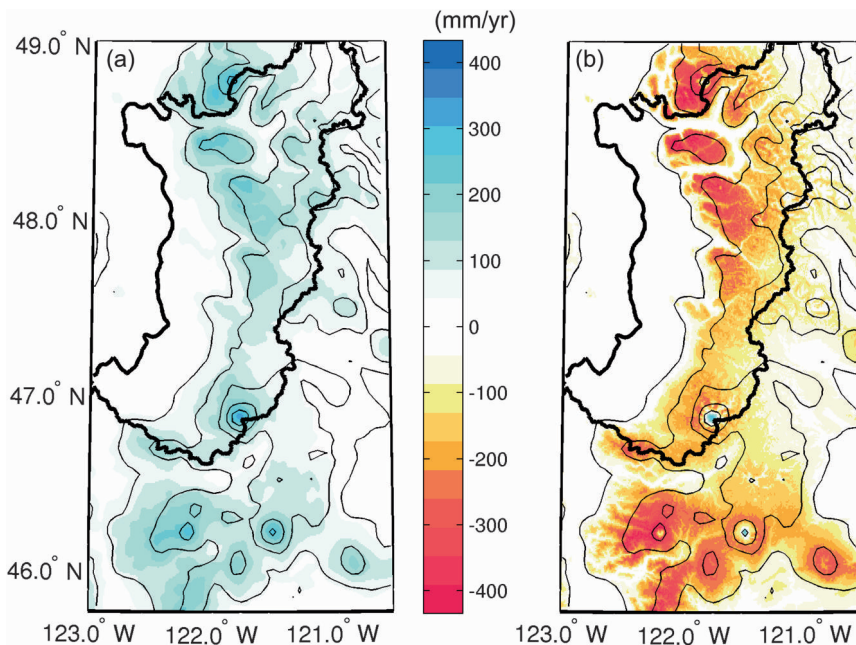


FIG. 3. Maps of LT model change in (a) precipitation and (b) snow water accumulation for *climo_control* simulation. Smoothed topography (from MM5) is contoured every 500 m.

because this study simulates annual-mean snowfall, whereas Casola et al. (2009) simulates 1 April snowpack. If increases in accumulation season melting with warming are negligible for the region (i.e., if $\lambda \sim \lambda_S$), then the models are in close agreement. However, if accumulation season melting increases substantially with warming (making λ larger in magnitude than λ_S), then the LT model underestimates the magnitude of λ and thus implies a more sensitive snowpack than Casola et al. (2009). In terms of how precipitation increases affect snowfall accumulation, the two studies agree. Casola et al. (2009) used temperature and precipitation data at a single representative station to estimate that only 76% of increased precipitation would translate into increased snowpack. This value is similar to the 82% from the LT snowfall model, a notable agreement because these estimates were attained by very different methods.

c. Sensitivity to the vertical structure of the warming

The LT snowfall model runs have used a vertical structure to climate warming that is determined by the assumption of constant moist stability, which has consequences for λ_S . These consequences are examined by analyzing the output of another LT model simulation where a 1°C warming that is uniform with elevation is assumed (Table 1, *climo_ΔTunif*). Although uniform temperature change would result in a change in N_m , it is held constant for LT model dynamics to focus on effects of ML changes and CC scaling.

Table 1 reveals significant differences in the estimate of λ_S depending upon the vertical profile of warming that is assumed. The simulation where ΔT is a function of elevation (*climo_control*) has a λ_S value of 3.3% °C⁻¹ larger in magnitude than when uniform warming is used (*climo_ΔTunif*). This difference arises from differences in λ_{ML} . The uniform and structured warming cases have similar temperature and ML changes at midelevations (near 1.5 km), where the most snow accumulates so that similar amounts of snow are lost due to ML changes. However, in calculating λ , the snowpack change is divided by the sea level ($z = 0$) warming, which is smaller in the *climo_control* case, leading to a λ_{ML} of larger magnitude. Here, λ_P is not similarly affected because it is controlled by the same surface temperature change used in the λ calculation.

4. ML model

The LT snowfall model considers a range of physical processes. To isolate those most fundamental for determining λ_S a simpler model, containing only minimal elements, is analyzed. This model just includes the distribution of topographic area with elevation and the climatological ML frequency distribution, and it is referred to as the ML model. Comparing this model with the LT model shows that the relationship between the ML frequency distribution and the mountain hypsometry is the predominant control on λ_S .

TABLE 1. Sensitivity of snow accumulation to warming for various runs of LT and ML models. The top section of the table gives results for the two long simulations (1980–2007), with and without vertical structure to the warming, discussed in sections 2 and 3. The lower section is for simulations of October–April 2005/06 and 2006/07 (acc0607) used for the experiments discussed in section 4. All values are in units of percent change in snow accumulation per degree Celsius of surface warming ($\% \text{ } ^\circ\text{C}^{-1}$). ML model entries that are left blank have the same value as exp_control.

Run	LT model			ML model		
	λ_{ML}	λ_P	λ_S	λ_{ML}	λ_P	λ_S
1980–2007						
climo_control	–22.6	5.49	–18.1	–25.1	6.84	–19.8
climo_ΔTunif	–19.4	5.55	–14.8	–21.6	6.84	–16.3
acc0607						
exp_control	–20.3	5.56	–15.6	–23.2	6.90	–17.7
exp_wdir50	–23.4	5.76	–18.7			
exp_τ850	–21.3	6.03	–16.3			
exp_ΔML_0	–23.6	5.60	–19.0	–25.7	6.90	–20.4
exp_ΔML_400	–18.2	5.51	–13.4	–22.2	6.90	–16.6
exp_Pbg0	–20.0	6.92	–14.2			
exp_PbgX2	–20.6	4.47	–16.8			
exp_PbgCC	–20.3	7.14	–14.3			
exp_z75%	–27.8	5.21	–23.8	–30.7	6.90	–25.6
exp_z125%	–15.9	5.79	–10.8	–18.5	6.90	–12.7
exp_x75%	–20.1	5.68	–15.3			
exp_x125%	–20.3	5.43	–15.8			

a. Methods

The ML model is based on three major simplifying assumptions: 1) atmospheric soundings during storms are representative of steady-state conditions for the 12 h that surround them; 2) during storms the precipitation rate is always the same constant and uniform value across the domain (i.e., there is no temporal or spatial variation in precipitation rate); and 3) the elevation at which a threshold temperature is reached in the sounding determines a uniform ML across the landscape.

The ML model has a similar degree of complexity as the geometric model of Casola et al. (2009). However, the ML model differs from Casola et al. (2009)'s model in that it requires no assumptions about the lapse rate, snow-base elevation, or snow-profile shape because these all come directly from climatological observations and physical considerations.

To formulate the ML model, the terrain is first binned by elevation bands (of size $\Delta z = 20$ m) to give the distribution of area with elevation $A(z)$ (Fig. 4a). The same MLs used in the LT model simulations (including the displacement ΔML) are then used to determine the climatological frequency distribution of storm MLs $f(ML; z)$, (Fig. 4b). From $f(ML; z)$ and the assumption of constant and uniform precipitation (with value P_o) the profile of snowfall $S(z)$ can be found by summing over the

climatological distribution of storm MLs, adding snowfall to all elevations above each ML. The corresponding expression for the climatological average snow accumulation S at each elevation z_N is

$$S(z_N) = P_o \sum_{i=1}^N f(ML; z_i) \Delta z \Delta t, \quad (3)$$

where elevation bins are indexed with $i = 1$ at sea level, and Δt is the interval of time associated with each sounding (12 h). Figure 4c shows the resulting $S(z)$ profile attained, assuming a P_o of 1 mm h^{-1} . Multiplying $A(z)$ by $S(z)$ gives the total volume of accumulated snow water in each elevation band $\Sigma(z)$ (Fig. 4d).

The ML model assumes that, under climate warming, temperature increases are uniform (i.e., 1°C at all elevations). In a warmed climate, the model simply increases the precipitation intensity according to the CC scaling as set by the mean temperature at the sounding's lowest level ($\sim 6.8\% \text{ } ^\circ\text{C}^{-1}$). Profiles for the warmed climate are shown in Fig. 4.

b. Results

Calculating λ_S for the ML model gives $-16.3\% \text{ } ^\circ\text{C}^{-1}$ (Table 1, climo_ΔTunif). Isolating the effects of ML changes, by holding precipitation constant, gives a λ_{ML} of $-21.6\% \text{ } ^\circ\text{C}^{-1}$, whereas isolating the effect of changes in precipitation intensity gives a λ_P of $6.84\% \text{ } ^\circ\text{C}^{-1}$ (Table 1, climo_ΔTunif). Note that these results do not depend on the value of P_o chosen because it cancels out in the fractional difference used to calculate the λ s. The ML model λ_S is within $2\% \text{ } ^\circ\text{C}^{-1}$ of the LT model value, and the models show a similar breakdown between λ_{ML} and λ_P (Table 1, climo_ΔTunif). Furthermore, in the ML model only 77% of the increased precipitation is realized as an increase in snowfall, similar to the 82% found for the LT model. An additional ML model simulation is also made using the low-level temperatures and MLs from the LT model runs where warming is a function of elevation, and the results from these simulations also agree well (Table 1, climo_control).

The ML and LT models are compared in more detail by examining profiles of change in $S(z)$ under warming for the climo_control runs (Fig. 5). The profiles reveal that the ML model is able to predict the distribution of snow loss with elevation well. This favorable comparison of the LT model and the very simple ML model suggests that the geometrical relationship between the ML distribution and the terrain—the only thing included in the ML model—dominates in setting the magnitude of λ_S . Spatial and temporal variations in orographic

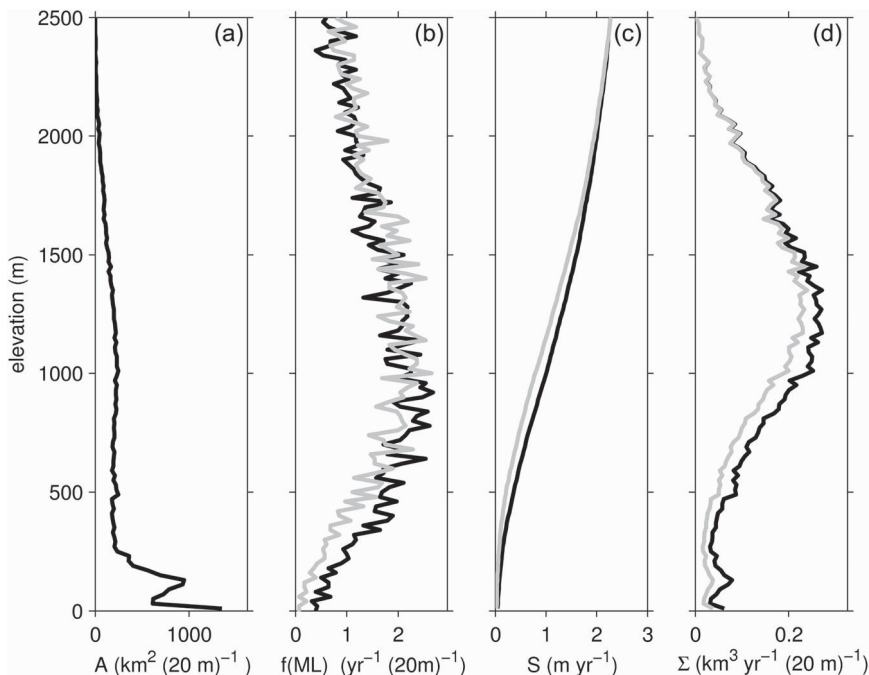


FIG. 4. Profiles of ML model variables for the Puget Sound catchment (Fig. 1) from the climo_ΔTunif run: (a) $A(z)$, (b) ML frequency distribution $f(\text{ML}; z)$, (c) $S(z)$, and (d) $\Sigma(z)$. Control simulation is shown in black, and warmed simulation is in gray.

precipitation are responsible for the differences between the two models. Although these variations have a quantitative impact on λ_S , they only make small modifications to the λ_S set by the elements included in the ML model.

5. Experiments: Controls on λ_S

Understanding how various aspects of both climate and topography control λ_S is key to understanding past and future changes in snowpack, uncertainties in projections of mountain snowpack, and the differing responses of mountain climates of the world to climate changes. Controls on λ_S are investigated by resimulating the snow accumulation seasons (October–March) of water years 2006–07 (acc0607) with the LT model, changing attributes of the incoming flow, model physics, and terrain. The control run for this period (Table 1, exp_control) uses the same configuration as climo_control, but produces a somewhat different λ_S , $-15.6\% \text{ } ^\circ\text{C}^{-1}$, due to interannual variability (Table 1). Although the following experiments reveal a range of ways in which climate and topography can affect λ_S , they also emphasize the importance of the relationship between mountain hypsometry and the ML climatology because only in experiments where these are significantly altered (for instance by changing the mean temperature or the mountain height) is λ_S substantially changed.

a. Climatic controls on λ_S

1) PRECIPITATION PATTERN

The importance of orographic precipitation patterns is quantified by making large changes to the precipitation patterns in the LT model runs. First, the precipitation patterns are altered by changing the wind direction (exp_wdir50). The acc0607 period is resimulated with the LT snowfall model, rotating the wind direction clockwise by 50° during each event for both the control and warmed case (Fig. 6a). This drastically different wind climatology changes the precipitation pattern and increases the orographic enhancement of precipitation (cf. Figs. 6a and A1b, described below in appendix A). The precipitation pattern is altered in a second experiment by varying the value of the microphysical time delay τ (exp_τ850). The acc0607 period is resimulated with τ decreased to 850 s, compared with 1800 s from exp_control (Fig. 6b). Comparing Figs. 6b and A1b shows large changes in the precipitation pattern associated with decreasing τ , most notably increases in precipitation spatial variability and maxima.

In both of these experiments, the precipitation changes substantially but λ_S is only modestly affected (Table 1). Why do these substantial changes in the precipitation pattern fail to have a large impact on λ_S ? The success of the geometric model of Casola et al. (2009) and the ML

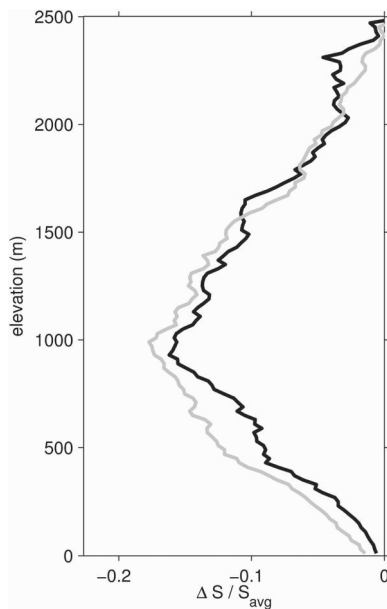


FIG. 5. Profile of change in $S(z)$ under climate warming from the ML model (gray) compared with the LT model (black). To facilitate comparison the $\Delta S(z)$ values from each model are normalized by dividing by the average of $S(z)$ from 0 to 2500 m for that model.

model (both essentially 1D) show that the shape of the $S(z)$ profile is central in setting λ_S . For $\text{exp}_{\tau 850}$ the profile of precipitation with elevation is changed very little (as shown in Fig. 7a), and thus the snow profile (Fig. 7b) and λ_S only changes modestly (Table 1). Larger changes to the precipitation and snow profiles occur for $\text{exp}_{\text{wdir}50}$ (Figs. 7a,b), however, these are still not enough to drastically change λ_S (Table 1). Because these drastic changes in the precipitation pattern only have small impacts on λ_S , it is unlikely that the LT model errors in precipitation [Fig. B1a, the primary errors relative to snowpack observations] have large influences on the results of this study.

2) ML DEPRESSION

The role of the distribution of snowfall, independent of the distribution of total precipitation, is investigated by varying ΔML . Simulations are conducted where ΔML is changed to 0 or to -400 m, yielding $\lambda_{S,S}$ values of -19.0% and -13.4% $^{\circ}\text{C}^{-1}$, respectively (Table 1, $\text{exp}_{\Delta ML_0}$ and $\text{exp}_{\Delta ML_{400}}$). These ML shifts have more impact than changes in precipitation patterns because they affect the base elevation of the $S(z)$ profile (Figs. 7d–f). This implies that the apparent overprediction of lowland snow fraction (Fig. B1c), roughly equivalent to an overprediction of $-\Delta ML$, may result in a modest underestimate of the magnitude of λ_S .

3) BACKGROUND PRECIPITATION

The importance of the chosen value of background or synoptic precipitation P_{bg} is investigated through runs with P_{bg} set to zero and doubled (results shown in Table 1, exp_{Pbg0} and exp_{PbgX2}). These reveal that λ_P decreases with increasing P_{bg} , causing λ_S to increase in magnitude. This results from the assumption that P_{bg} does not change with temperature. Because P_{bg} is constant with climate, larger values of P_{bg} relative to total precipitation lead to more modest fractional increases in precipitation and larger fractional losses of snow. If, alternatively, P_{bg} is made to scale with the increasing atmospheric moisture (as determined by the CC scaling with surface temperatures; Table 1, exp_{PbgCC}), λ_P increases to 7.14% $^{\circ}\text{C}^{-1}$, roughly the value for the $P_{bg} = 0$ case.

4) MEAN TEMPERATURE

The importance of mean temperature is quantified by estimating the λ_S that the Cascades would have were it subject to substantially warmer or colder climate. This is done with a series of simulations, with both models, of the acc0607 period where the incoming flow is warmed or cooled by various amounts while maintaining constant N_m . The sounding temperatures at 1.5 km are changed by $\pm 0.5^{\circ}$, 1° , 2° , 4° , 6° , and 10°C , with corresponding sea level changes of $\pm 0.41^{\circ}$, 0.83° , 1.66° , 3.31° , 4.98° , and 8.33°C , respectively. The output from these simulations is used to calculate λ_S values by taking centered fractional differences of $\Sigma_r(T)$. The results in Fig. 8 show the range of sensitivities that would be expected for a Cascade-like mountain range in warmer and cooler climates. For a 4°C warmer climate, λ_S is approximately doubled in magnitude and for a 7°C -cooler climate it is reduced to zero. Figure 8 also shows that the basic temperature dependence of λ_S is well captured by the ML model (except at much cooler temperatures, where the treatment of non-orographic lowland snow causes large differences), as it is mainly determined by where the distribution of MLs lies on the mountain.

b. Topographic controls on λ_S

1) BASIN-TO-BASIN VARIABILITY

Differences in λ_S between the major catchments of the study region (distinguished in Fig. 1) are considered. Figure 9 shows that values of λ_S estimated by the LT snowfall model plotted against the values estimated by the ML model. For these basins λ_S ranges from -14% to -32% $^{\circ}\text{C}^{-1}$, revealing that different portions of the Cascades, subject to the same regional climate but different topography, exhibit considerable variability in their response to warming. This is due largely to the differing hypsometries of these basins relative to the ML

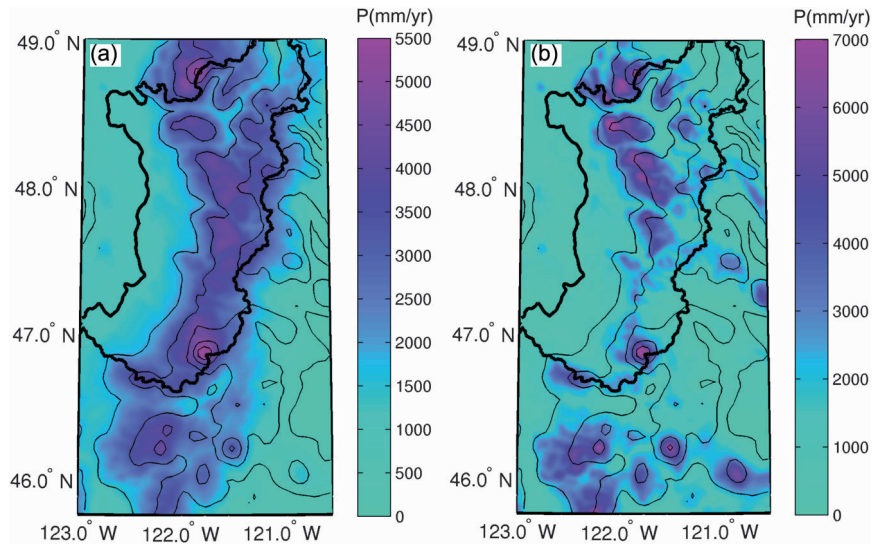


FIG. 6. LT model simulated precipitation patterns (mm yr^{-1}) for acc0607 period from runs with (a) more westerly wind direction ($\text{exp_}\Delta\text{wdir50}$), and (b) decreased microphysical time delay ($\text{exp_}\tau\text{850}$). MM5 topography is contoured every 500 m.

distribution, evidenced by the ML model’s ability to capture variations in λ_S . Note that basin-to-basin variability is quite large in comparison with the effects of most climate factors (e.g., the scaling of precipitation, vertical structure of the warming, and ΔML).

2) MOUNTAIN HEIGHT AND WIDTH

To investigate the importance of mountain height, the acc0607 period is resimulated with the topographic height scaled by a uniform factor of 75% or 125%. As the scale

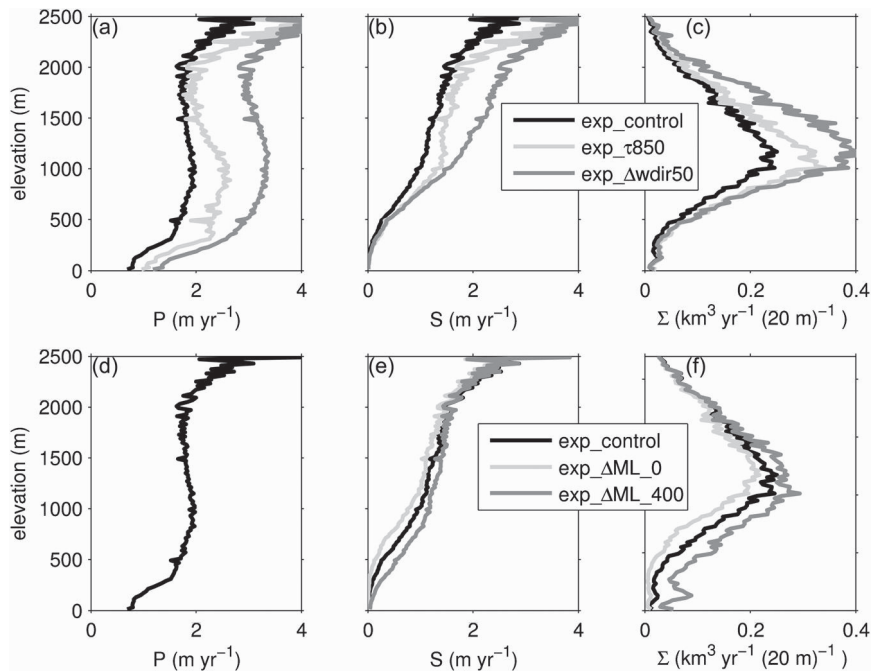


FIG. 7. (a)–(c) Profiles of LT snowfall model $P(z)$, $S(z)$, and $\Sigma(z)$ for acc0607 period from (black) exp_control , (light gray) $\text{exp_}\tau\text{850}$ ($\text{exp_}\tau\text{850}$) experiment, and (dark gray) $\text{exp_}\Delta\text{wdir50}$ experiment. (d)–(f) As in (a)–(c), but for (black) exp_control , (light gray) $\text{exp_}\Delta\text{ML}_0$, and (dark gray) $\text{exp_}\Delta\text{ML}_{400}$.

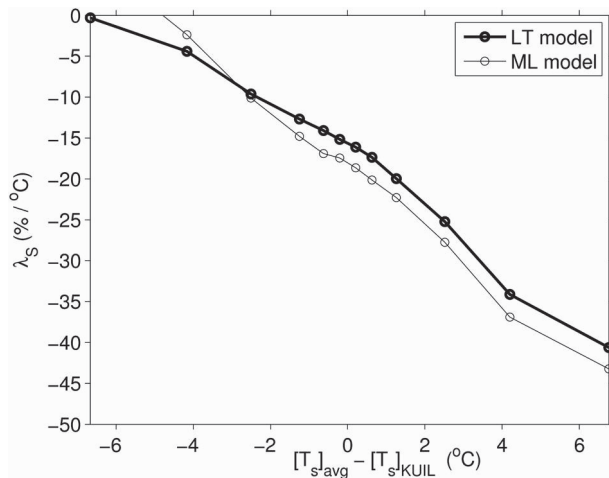


FIG. 8. Values of λ_S estimated as a function of average sea level temperature during storms. Temperatures are relative to current KUIL climatology $[(T_s)_{\text{avg}} - (T_s)_{\text{KUIL}}$, with $(T_s)_{\text{KUIL}} = 8.5^\circ\text{C}$]. Thick line is for LT model, and thin line is for ML model.

is reduced there is a decrease in orographic precipitation due to a reduced lifting of the incoming flow, and also a decrease in snow versus rain due to an increased fraction of the terrain residing below the storm MLs (Table 1, *exp_z75%* and *exp_z125%*). Unsurprisingly, the temperature sensitivity decreases in magnitude as mountain height is increased and more of the mountain is subject to cold temperatures, with λ_S going from -23.8% to $-10.8\% \text{ } ^\circ\text{C}^{-1}$. This is largely because of changes in λ_{ML} , which goes from -27.8% to $-15.9\% \text{ } ^\circ\text{C}^{-1}$. With increased mountain height, λ_P also changes, increasing from 5.21% to $5.79\% \text{ } ^\circ\text{C}^{-1}$, and the fraction of the precipitation increase realized as snow increases from 77% to 88%.

The importance of mountain width is investigated by resimulating the *acc0607* period using the LT model with the east–west dimensions of the model grid cells scaled by 75% or 125%. As the mountain narrows the total precipitation integrated over the windward slope decreases somewhat (due to more spillover and leeside evaporation of precipitation), but the average precipitation at each elevation increases because the rain and snowfall is distributed over a smaller area. However, these changes do little to alter the shape of the $S(z)$ profile (not shown) and, as a result, barely affect the values of λ_S (Table 1, *exp_x75%* and *exp_x125%*).

c. Response to warming in excess of 1°C

So far this study has only dealt with the changes in snowpack associated with a 1°C warming. Results have been expressed as a percentage change in snow accumulation per degree of warming, units which imply the

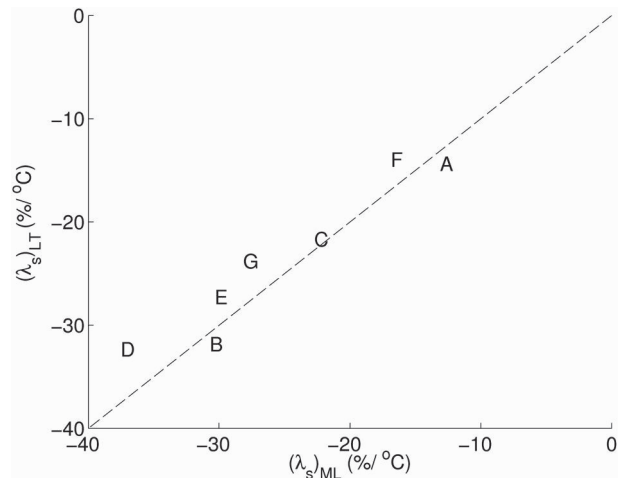


FIG. 9. Sensitivity of snowfall to warming predicted by the LT snowfall model $(\lambda_S)_{\text{LT}}$ vs sensitivity from the ML $(\lambda_S)_{\text{ML}}$ for various catchments draining into Puget Sound (indicated with letters in Fig. 1). The dashed line has a slope of unity for comparison. Note the large basin-to-basin variability of λ_S exhibited by both models.

fractional loss of snowpack scales linearly with the amount of warming, but this may not be the case. To investigate how the magnitude of the climate warming determines the loss of snowfall, the experiments described in section 5a(4) are used to calculate fractional changes in snow accumulation (relative to the control climate) as a function of sea level temperature change, ΔT_s (Fig. 10).

This analysis reveals that for surface warming up to $\sim 4^\circ\text{C}$ the fractional loss of snow is an approximately linear function of ΔT_s , which can be estimated well from the $\Delta T = 1^\circ\text{C}$ case (see fine dashed line in Fig. 10). Also shown is how the change in snowfall because of precipitation changes or ML changes alone depends on the amount of warming (gray lines in Fig. 10). This demonstrates that the relative importance of precipitation and ML changes is a strong function of the amount of warming. Figure 10 also shows that for large amounts of warming, the loss of accumulation area due to ML changes dominates and precipitation changes have a negligible effect. This is emphasized by comparison of the total loss in accumulation with the loss predicted by summing the ML and precipitation related changes (solid and dashed black lines in Fig. 10). For modest amounts of warming these two values are similar because much of the increase in precipitation is realized as an increase in snowfall. However, for large amounts of warming the total loss of snowfall is much greater than the sum of the two effects because much of the increase in precipitation occurs in areas where snow has been turned to rain as MLs rise. For surface warming in excess of approximately

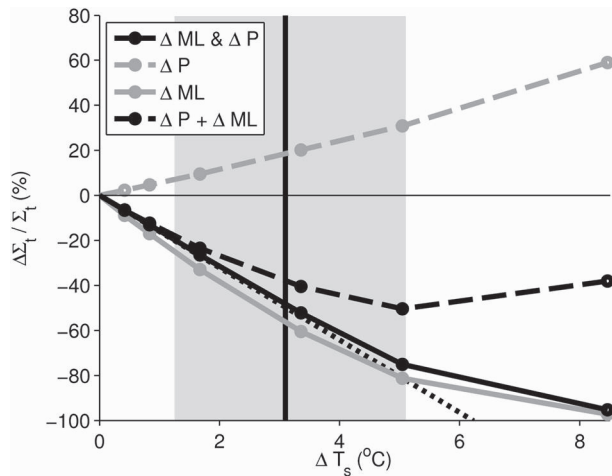


FIG. 10. Percentage change in snow accumulation as a function of surface warming, as estimated by LT snowfall model (black solid line, with circles showing individual model runs). Gray solid line and dashed lines show the changes that would occur if only MLs or precipitation intensity were to change with warming. Black dashed line shows the sum of the two gray lines. The fine dashed line shows the linear extrapolation of the λ_S values calculated from the $\Delta T = 1^\circ\text{C}$ case. The shaded region shows the range of GCM projected warmings (for 2080s minus 1980s) for the Pacific Northwest region (Climate Impacts Group 2009). Projections come from the IPCC AR4 models with emissions scenario A1B. Vertical line shows the best GCM estimate attained from a weighted average of the AR4 models (Climate Impacts Group 2009).

2°C , less than 50% of the precipitation increase adds to the snowpack, and for 5°C this is reduced to less than 20%. Therefore, under substantial warming the loss of snow accumulation area provides a profound limit on how much precipitation increases may act to preserve the snowpack.

Figure 10 also shows the range and “best guess” of wintertime warming projected for the northwestern United States from the Intergovernmental Panel on Climate Change (IPCC) Fourth Assessment Report (AR4) GCMs for the 2080s relative to the 1980s (Climate Impacts Group 2009). Taking into account this range of projections, the LT snowfall model suggests a very large uncertainty in the amount of snowfall loss by late in the century: 20%–75%. This range comes from uncertainties in how greenhouse gas emissions relate to regional climate warming. For the LT snowfall model these uncertainties appear much larger than those associated with the choice of methods and model parameters used to relate a given warming to a change in snow accumulation (note the range of λ_S values in Table 1). The loss of snowfall is substantial even at 3°C , in the middle of the range of possible warmings, despite an almost 20% increase in precipitation because much of the precipitation increase is lost to runoff.

d. Response to circulation changes

The LT snowfall model may also be used to assess the importance of climate changes other than warming. It has been suggested that circulation changes associated with global warming may cause winds to impinge against the Cascades at a different angle, resulting in altered orographic enhancement of precipitation (Salathé et al. 2008; Climate Impacts Group 2009). The importance of such circulation changes are roughly quantified by re-running the LT snowfall model assuming that, in addition to warming, climate change includes a shift in the wind direction during storms. An experiment is conducted where the acc0607 period is resimulated with the winds shifted clockwise by 12° (an amount equal to twice the standard deviation of the annual-mean wind direction in the 1–2-km layer of the KUIL storm soundings). This shift makes the winds more perpendicular to the Cascades and increases orographic enhancement. The increase in orographic precipitation due to the wind shift almost perfectly cancels out the loss of snow due to warming, resulting in a decrease in snowfall of only -0.5% for 1°C of surface warming (instead of -15.6% in the control case). Note that this method neglects the effect that circulation changes would have on the temperature and moisture characteristics of the incoming flow. More westerly winds would presumably be colder and drier. Thus, these results likely overestimate the impact of circulation changes, perhaps presenting an effective upper limit. If instead the winds are rotated counterclockwise by 12° , there is reduced orographic enhancement and an increased snowfall loss of -29.9% . These results suggest that if regional climate change includes substantial shifts in circulation patterns, then the associated changes in orographic enhancement may be important for snowpack, possibly more important than precipitation changes directly due to warming.

6. Conclusions

Controls on the sensitivity of mountain snowpack accumulation to climate warming λ_S have been examined using experiments with a pair of idealized, physically based models: an idealized orographic snowfall model (the LT snowfall model), and a very simple melting-level (ML) model. Experiments and comparisons between the two models show that the relationship between the climatological distribution of storm MLs and the mountain hypsometry is the strong underlying determinant of λ_S .

Accounting for ML changes alone, the more sophisticated of these two models gives a temperature sensitivity of -19.4% or -22.6% $^\circ\text{C}^{-1}$ of warming for the

windward slopes of the Washington Cascades, depending on the vertical structure of the warming. For modest amounts of warming, increases in orographic precipitation associated with increasing atmospheric moisture may play an important role in moderating the loss of snowfall, reducing the magnitude of the Cascades sensitivity to -14.8% or -18.1% $^{\circ}\text{C}^{-1}$. However, for the Cascades, and presumably other temperate mountains of moderate height, once the warming exceeds a few degrees physically plausible increases in orographic precipitation are unable to compete with the loss of accumulation area and have minimal effects on λ_S . Shifts in circulation patterns may also play an important role. Changes in wind direction have large impacts on the intensity of orographic precipitation and accordingly may act to moderate or exacerbate the loss of mountain snowpack under climate change.

Because λ_S is determined mainly from the terrain and ML distribution, simple models such as the ML model and Casola et al. (2009)'s geometrical model can be quite effective tools for estimating λ_S . The ML model is computationally cheap, requires minimum input data, and compares favorably with more complex models. Thus it may be useful for resource managers desiring ballpark estimates of the vulnerability of specific mountainous watersheds to climate warming. It is more generally applicable than the geometrical model of Casola et al. (2009) because it does not require assumptions about the base elevation of the snowpack, the shape of the snow profile, or the lapse rate.

By focusing on identifying the relative importance of various factors for determining λ_S , this research offers information about what models must capture to make realistic projections of the impacts of warming on mountain snowpack. For instance, large differences in the climatological pattern of orographic precipitation were found to have only modest effects on λ_S . Thus, biases in precipitation patterns in regional climate models may not introduce large errors in projections of fractional snowpack change. In contrast, the distribution of MLs relative to the basin hypsometry is of fundamental importance. Accordingly, differences in the hypsometry of adjacent catchments in the same mountain range may lead to substantial differences in λ_S , and errors in characterizing MLs may have sizeable effects on estimates of λ_S .

Many results of this study should be broadly applicable to other mid- and high-latitude mountain ranges around the world that receive much of their precipitation during moist, stable, and relatively unblocked flow. Experiments where mountain shape and mean temperature are varied give a sense of how results may be different for mountains with different terrain geometry or mean climate. Despite these differences, the importance

of hypsometry and ML climatology and the decreasing importance of precipitation changes with increasing warming should hold true for many other regions.

Acknowledgments. Gerard Roe, Jessica Lundquist, Dale Durran, and Sandra Penny all provided valuable comments and suggestions that improved the manuscript. Joe Casola assisted in the processing of the SNOTEL data. The archived fifth-generation Pennsylvania State University–National Center for Atmospheric Research Mesoscale Model (MM5) forecasts were provided by the Northwest Regional Modeling Consortium. This work was supported by a National Science Foundation (NSF) Graduate Research Fellowship and NSF Grant EAR-0642835.

APPENDIX A

LT Snowfall Model Calibration

The LT snowfall model is calibrated by comparing its output with that of an operational mesoscale weather forecast model, adjusting the τ , P_{bg} , and ΔML parameters to maximize the agreement between the two. Simulated precipitation from the MM5 modeling system run operationally by the Northwest Regional Modeling Consortium at the University of Washington (Mass et al. 2003) is used. The MM5 was run twice daily with horizontal resolution of 4 km over the Cascade Mountains from 1997 to 2008 (a full listing of the model grid, initialization, and parameterization choices are available online at <http://www.atmos.washington.edu/mm5rt/>).

The precipitation simulated from forecast hours 24–36 of each MM5 run for the snow accumulation season of two water years (October–March of 2005/06 and 2006/07) was integrated over all forecasts to find the mean precipitation (as in Anders et al. 2007; Minder et al. 2008). Figure A1 shows maps of mean accumulation season precipitation simulated by MM5 and the LT model, and Fig. A2 shows vertical profiles of average precipitation as a function of elevation. A P_{bg} of 0.25 mm h^{-1} and a τ of 1800 s were chosen by trial and error to subjectively maximize agreement between the mean precipitation profiles and maps for the two models. Figures A1 and A2 show that the vertical profile of precipitation and the basic pattern of orographic enhancement are similar between the two models. Differences occur in terms of how much precipitation is simulated at mid-to-high elevations and in the northeast corner of the domain. Yet, overall the LT model produces a plausible simulation of precipitation that includes the primary features present in the MM5 forecasts.

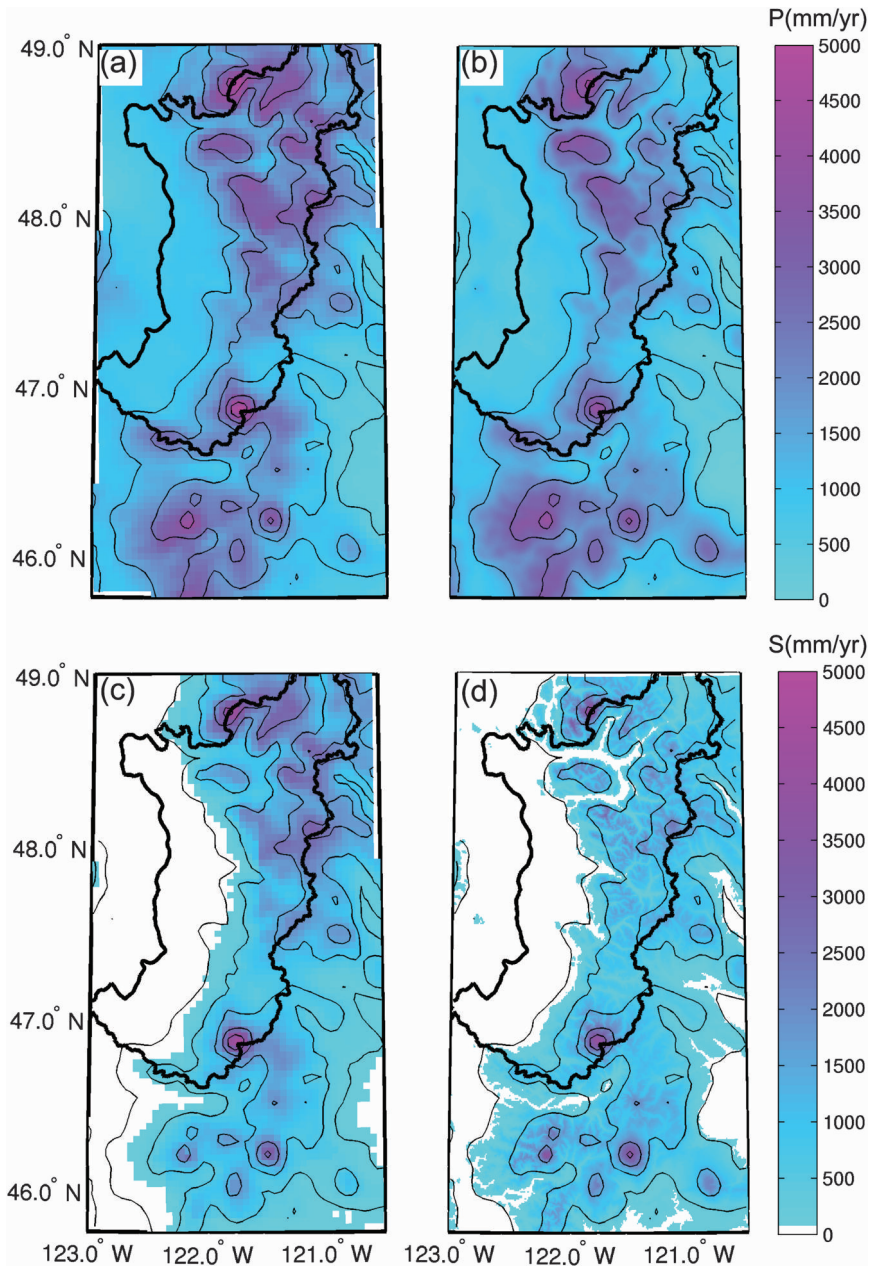


FIG. A1. Comparison of maps of P and S from MM5 and LT models for October–March 2005/06 and 2006/07: (a) MM5 modeled P , (b) LT modeled P , (c) MM5 modeled S , (d) LT modeled S . Thick black line shows the Puget Sound catchment. The MM5 elevation is contoured with thin black lines every 500 m.

Comparing snowfall simulated by the two models is less straightforward because snow accumulation is not an archived field for the MM5 forecasts. To approximate MM5 snowfall, the modeled 2-m temperatures are used with a 1°C temperature threshold to estimate the phase of modeled precipitation at each grid cell for each 12 h (results shown in Figs. A1 and A2). A ΔML of -200 m was chosen to match the mean snowfall profiles from the

two models. The LT snowfall model reproduces the basic structure of the MM5 snowfall profile. The most notable difference between the two models is that there is less snow above 1000 m in the LT snowfall model. This is due in part to less precipitation at these elevations and in part to more rain versus snow in the LT model. However, because the MM5 snowfall is only crudely estimated, and may have its own biases, it is unclear how

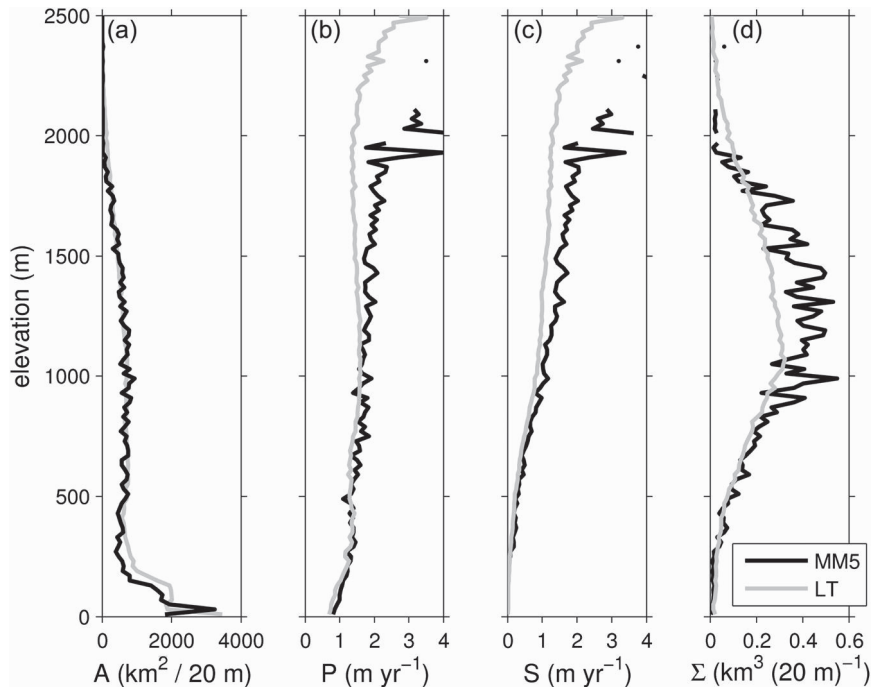


FIG. A2. Comparison of LT model and MM5. Profiles of (a) $A(z)$, (b) $P(z)$, (c) $S(z)$, and (d) $\Sigma(z)$ from MM5 (black line) and LT snowfall model (gray line) for the accumulation seasons of water years 2006 and 2007. Profiles are evaluated for the entire domain shown in Fig. A1.

significant this difference is. Furthermore, appendix B shows that there does not appear to be a systematic underprediction of high-elevation snow in the LT model when it is compared with station observations.

APPENDIX B

LT Snowfall Model Evaluation

The LT snowfall model is evaluated by comparing its simulation of annual-mean snowfall with that measured by the SNOTEL network of automated snow observations (available online at <http://www.wcc.nrcs.usda.gov/snow/>). For a collection of SNOTEL stations in the model domain with long records (shown in Fig. 1) daily observations are used to calculate the mean October–April accumulated snow S and precipitation P for the SNOTEL period of record (1980–2007). Only daily gains in snow are summed, neglecting days with snow loss, to evaluate S . For each station the LT precipitation is linearly interpolated to the station location and the actual station elevation is used with the model ML for the determination of precipitation phase. For all water years with available data the fractional error in the simulated P and S , $(forecast - observation)/observation$, is calculated and presented as a function of elevation (Figs. B1a,b).

The mean absolute fractional error is 0.33 for P and 0.40 for S . Spatial correlation coefficients are 0.53 for P and 0.52 for S . The errors that occur at many sites are unsurprising because orographic precipitation has proven challenging to simulate, even with sophisticated models (e.g., Colle et al. 2000). Furthermore, the significance of the errors is unclear because site-specific factors (e.g., vegetation, aspect) and observational biases (e.g., gauge undercatch, snow drift) may affect SNOTEL observations, and substantial errors can occur even for a perfect model when comparing gridcell predictions to point observations (e.g., Tustison et al. 2001). Nevertheless, the absence of large systematic biases or distinct vertical structure in the error is encouraging. The possible impact of model biases on λ_S estimates is discussed in section 5a(1).

The ability of the LT snowfall model to reproduce the observed partitioning between rain and snow is also evaluated by calculating and comparing the average ratio of October–April accumulated S to P for model and observations (Fig. B1c). This shows that, except for the lowest elevation stations, the model reproduces the observed snowfall fraction (with a mean absolute fractional error of 0.14 and spatial correlation of 0.88) quite well, meaning that the simple model of the rain–snow transition used works reasonably well and that errors in S are primarily due to errors in P .

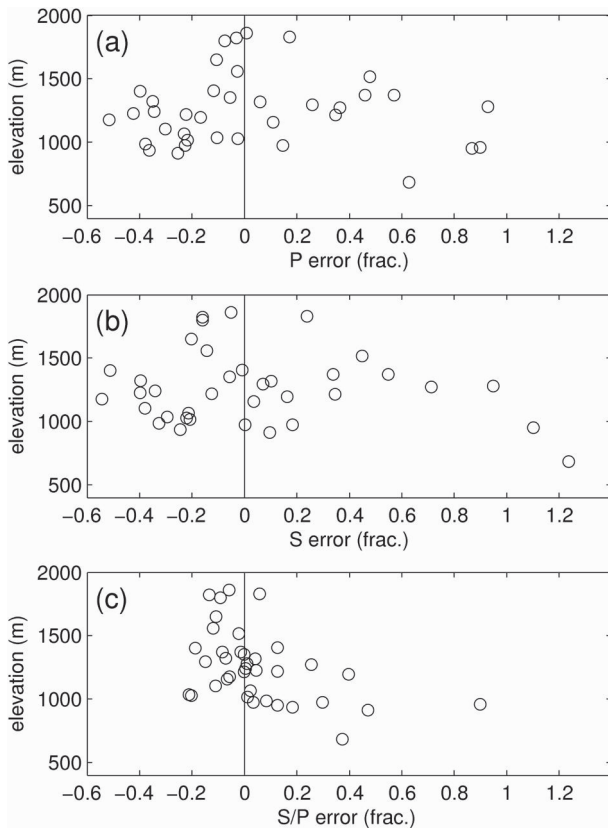


FIG. B1. Comparison of LT snowfall model with SNOTEL observations. Average fractional error in LT modeled October–April (a) P and (b) S accumulation, and (c) S/P relative to SNOTEL stations as a function of elevation for 1980–2007.

REFERENCES

- Anders, A. M., G. H. Roe, D. R. Durran, and J. R. Minder, 2007: Small-scale spatial gradients in climatological precipitation on the Olympic Peninsula. *J. Hydrometeorol.*, **8**, 1068–1081.
- Barnett, T. P., J. C. Adam, and D. P. Lettenmaier, 2005: Potential impacts of a warming climate on water availability in snow-dominated regions. *Nature*, **438**, 303–309.
- Barstad, I., and R. B. Smith, 2005: Evaluation of an orographic precipitation model. *J. Hydrometeorol.*, **6**, 85–99.
- Beniston, M., F. Keller, B. Koffi, and S. Goyette, 2003: Estimates of snow accumulation and volume in the Swiss Alps under changing climatic conditions. *Theor. Appl. Climatol.*, **76**, 125–140.
- Casola, J., L. Cuo, B. Livneh, D. Lettenmaier, M. Stoelinga, P. Mote, and J. Wallace, 2009: Assessing the impacts of global warming on snowpack in the Washington Cascades. *J. Climate*, **22**, 2758–2772.
- Cayan, D. R., 1996: Interannual climate variability and snowpack in the western United States. *J. Climate*, **9**, 928–948.
- Climate Impacts Group, 2009: *The Washington Climate Change Impacts Assessment: Evaluating Washington's Future in a Changing Climate*. University of Washington, 414 pp.
- Colle, B. A., C. F. Mass, and K. J. Westrick, 2000: MM5 precipitation verification over the Pacific Northwest during the 1997–99 cool seasons. *Wea. Forecasting*, **15**, 730–744.
- Crochet, P., T. Johannesson, T. Jonsson, O. Sigurdsson, H. Bjornsson, F. Palsson, and I. Barstad, 2007: Estimating the spatial distribution of precipitation in Iceland using a linear model of orographic precipitation. *J. Hydrometeorol.*, **8**, 1285–1306.
- Dai, A. G., 2008: Temperature and pressure dependence of the rain–snow phase transition over land and ocean. *Geophys. Res. Lett.*, **35**, L12802, doi:10.1029/2008GL033295.
- Durran, D. R., and J. B. Klemp, 1982: On the effects of moisture on the Brunt–Väisälä frequency. *J. Atmos. Sci.*, **39**, 2152–2158.
- Frierson, D. M. W., 2006: Robust increases in midlatitude static stability in simulations of global warming. *Geophys. Res. Lett.*, **33**, L24816, doi:10.1029/2006GL027504.
- Hamlet, A. F., and D. P. Lettenmaier, 1999: Effects of climate change on hydrology and water resources in the Columbia River basin. *J. Amer. Water Resour. Assoc.*, **35**, 1597–1623.
- , P. W. Mote, M. P. Clark, and D. P. Lettenmaier, 2005: Effects of temperature and precipitation variability on snowpack trends in the western United States. *J. Climate*, **18**, 4545–4561.
- Held, I. M., and B. J. Soden, 2006: Robust responses of the hydrological cycle to global warming. *J. Climate*, **19**, 5686–5699.
- Howat, I. M., and S. Tulaczyk, 2005: Climate sensitivity of spring snowpack in the Sierra Nevada. *J. Geophys. Res.*, **110**, F04021, doi:10.1029/2005JF000356.
- Kirshbaum, D., and R. Smith, 2008: Temperature and moist-stability effects on midlatitude orographic precipitation. *Quart. J. Roy. Meteor. Soc.*, **134**, 1183–1199.
- Knowles, N., M. D. Dettinger, and D. R. Cayan, 2006: Trends in snowfall versus rainfall in the western United States. *J. Climate*, **19**, 4545–4559.
- Leung, L. R., and Y. Qian, 2003: The sensitivity of precipitation and snowpack simulations to model resolution via nesting in regions of complex terrain. *J. Hydrometeorol.*, **4**, 1025–1043.
- Lundquist, J., P. Neiman, B. Martner, A. White, D. Gottas, and F. Ralph, 2008: Rain versus snow in the Sierra Nevada, California: Comparing Doppler profiling radar and surface observations of melting level. *J. Hydrometeorol.*, **9**, 194–211.
- Marwitz, J. D., 1987: Deep orographic storms over the Sierra Nevada. Part I: Thermodynamic and kinematic structure. *J. Atmos. Sci.*, **44**, 159–173.
- Mass, C. F., and Coauthors, 2003: Regional environmental prediction over the Pacific Northwest. *Bull. Amer. Meteor. Soc.*, **84**, 1353–1366.
- Medina, S., B. F. Smull, R. A. Houze, and M. Steiner, 2005: Cross-barrier flow during orographic precipitation events: Results from MAP and IMPROVE. *J. Atmos. Sci.*, **62**, 3580–3598.
- Minder, J., D. Durran, G. Roe, and A. Anders, 2008: The climatology of small-scale orographic precipitation over the Olympic Mountains: Patterns and processes. *Quart. J. Roy. Meteor. Soc.*, **134**, 817–839.
- Mote, P. W., 2006: Climate-driven variability and trends in mountain snowpack in western North America. *J. Climate*, **19**, 6209–6220.
- , A. F. Hamlet, M. P. Clark, and D. P. Lettenmaier, 2005: Declining mountain snowpack in western North America. *Bull. Amer. Meteor. Soc.*, **86**, 39–49.
- , —, and E. Salathé, 2008: Has spring snowpack declined in the Washington Cascades? *Hydrol. Earth Syst. Sci.*, **12**, 193–206.
- Pierce, D., and Coauthors, 2008: Attribution of declining western U.S. snowpack to human effects. *J. Climate*, **21**, 6425–6444.
- Salathé, E., R. Steed, C. Mass, and P. H. Zahn, 2008: A high-resolution climate model for the U.S. Pacific Northwest: Mesoscale feedbacks and local responses to climate change. *J. Climate*, **21**, 5708–5726.

- Sawyer, J., 1956: The physical and dynamical problems of orographic rain. *Weather*, **11**, 375–381.
- Serreze, M. C., M. P. Clark, R. L. Armstrong, D. A. McGinnis, and R. S. Pulwarty, 1999: Characteristics of the western United States snowpack from snowpack telemetry (SNOTEL) data. *Water Resour. Res.*, **35**, 2145–2160.
- Smith, R. B., 1979: The influence of mountains on the atmosphere. *Adv. Geophys.*, **21**, 87–230.
- , and I. Barstad, 2004: A linear theory of orographic precipitation. *J. Atmos. Sci.*, **61**, 1377–1391.
- , Q. F. Jiang, M. G. Fearon, P. Tabary, M. Dorninger, J. D. Doyle, and R. Benoit, 2003: Orographic precipitation and air mass transformation: An Alpine example. *Quart. J. Roy. Meteor. Soc.*, **129**, 433–454.
- Stoelinga, M. T., M. D. Albright, and C. F. Mass, 2010: A new look at snowpack trends in the Cascade Mountains. *J. Climate*, **23**, 2473–2491.
- Tebaldi, C., K. Hayhoe, J. M. Arblaster, and G. A. Meehl, 2006: Going to the extremes. *Climatic Change*, **79**, 185–211.
- Tustison, B., D. Harris, and E. Foufoula-Georgiou, 2001: Scale issues in verification of precipitation forecasts. *J. Geophys. Res.*, **106**, 11 775–11 784.
- U.S. Army Corps of Engineers, 1956: *Snow Hydrology: Summary Report of the Snow Investigations*. North Pacific Division, U.S. Army Corps of Engineers, 437 pp.
- Vicuna, S., E. P. Maurer, B. Joyce, J. A. Dracup, and D. Purkey, 2007: The sensitivity of California water resources to climate change scenarios. *J. Amer. Water Resour. Assoc.*, **43**, 482–498.